

## Original Research Article

# Fabrication of a biodegradable scaffold with localized response to bacterial infections

Ammar M. Hassanbhai<sup>1</sup>, Jing Lim<sup>1</sup>, Feng Wen<sup>1</sup>, Heng Li Chee<sup>1</sup>, Bow Ho<sup>2</sup>, Mark S.K. Chong<sup>1</sup> and Swee Hin Teoh<sup>1,3\*</sup>

### Abstract

**Implant-associated infections remain a significant source of morbidity in the clinic. Systemic administration of antibiotics is often ineffective, due in part to limited vascularization of the implant site. Here, we describe a physical method of incorporating antibiotics into biodegradable scaffolds. Antibiotics gentamicin sulfate (GS) and metronidazole (MZ) were cryomilled with polycaprolactone (PCL) and subsequently heat-melted. Antibiotic-loaded films were evaluated for mechanical properties, drug release characteristics, anti-microbial efficacy and cytotoxicity. Our results suggest this process to be feasible for the generation of thin film coatings with varying drug concentrations. Release profiles indicated an initial burst release for both antibiotics with a sustained release of 3 and 8 days for GS and MZ films respectively. The films inhibited bacterial growth, while viability assays suggest low mammalian cytotoxicity. Taken together, these findings establish this method as a chemical-free means to form biodegradable drug scaffolds for the tailored local delivery of antibiotics.**

**Keywords:** Polycaprolactone, Cryomilling, Antimicrobial, Antibiotic delivery system, Implant-associated infections

<sup>1</sup>School of Chemical and Biomedical Engineering, Nanyang Technological University, Block N1.2, 62 Nanyang Drive, Singapore 637459

<sup>2</sup>Department of Microbiology, Yong Loo Lin School of Medicine, National University of Singapore, Singapore, Singapore

<sup>3</sup>Director, Centre for Bone Tissue Engineering, School of Chemical and Biomedical Engineering, Lee Kong Chian School of Medicine Senior Renaissance Engineering Programme (REP) Fellow  
Nanyang Technological University, N1.3-B5-01a, 62 Nanyang Drive, S637459.  
Chief Engineer, Skin Research Institute of Singapore (SRIS), 11 Mandalay Rd, Singapore 308232

\*Corresponding Author's E-mail: [teohsh@ntu.edu.sg](mailto:teohsh@ntu.edu.sg)

## INTRODUCTION

Implant associated infections present a major problem in the clinics. In orthopaedic surgeries, for example about 22% of revision operations arose due to infections (Coello et al., 2005), where common complications include acute or chronic osteomyelitis caused by bacteria and soft tissue-related infections around the site of trauma (Hui et al., 2009). Furthermore, these infections are a major source of site morbidity, resulting in compromised clinical outcomes and increased mortality risks (Ragel and Vallet-Regi, 2000). Standard of care treatment includes traditional systemic antibiotic regimens if unsuccessful may be followed by implant removal and/or tissue debridement (Lucke et al., 2003). However, these treatments are sub-optimal, as the infections are difficult to eliminate and treat due to patient and associated-pathogenic factors. This is especially so at avascular wound sites that suffer from compromised biodistribution and the attendant complications, including a need for elevated drug doses to ensure efficacy at the infection site and also the development of antibiotic-resistant strains (Coello et al., 2005; Murray et al., 2006;

Aronson et al., 2006; Noel et al., 2008). Efforts to improve this approach include replacing the infected implants with bone void fillers adsorbed with antibiotics (as off-label applications), antibiotic-infused collagen sponges, or antibiotic-impregnated bone cement (Lucke et al., 2003), that would release antibiotics for a prolonged duration for an interim period prior to final replacement with a new implant. These inefficient treatment regimens place a major burden on the patient due to the high costs of multiple procedures involved and the prolonged pain and suffering they have to endure. To avoid these issues, several groups have proposed the sustained local release of prophylactic antibiotics from the implants (Ragel and Vallet-Regi, 2000). Such local treatment is generally preferred over systemic administration for reasons of increased bioavailability, sustained concentrations near the minimal effective concentrations and avoidance of systemic dose toxicity of the antibiotic (Bailey, 1997).

Within the last decade, numerous pharmaceutical studies have demonstrated the use of bioresorbable

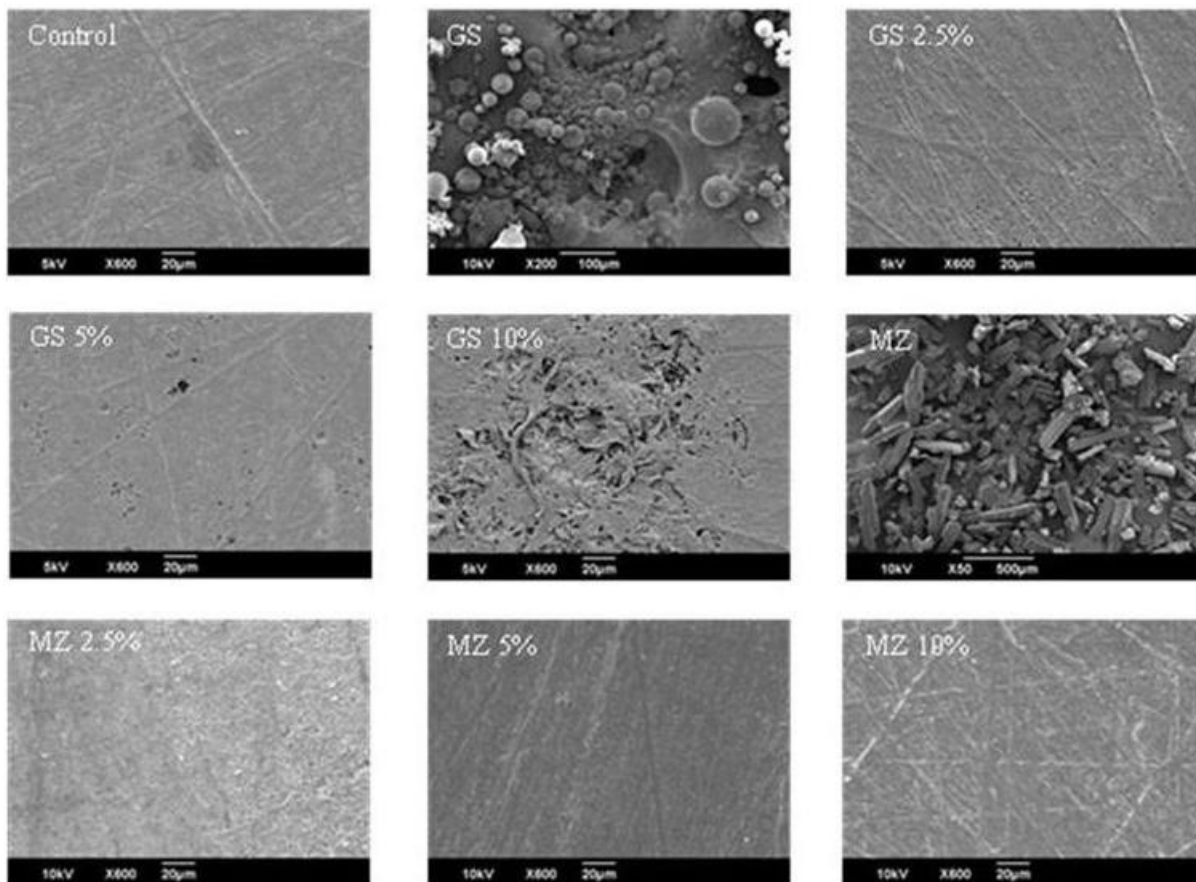


**Figure 1.** SEM images of control (PCL), GS / MZ powder and PCL-GS / PCL-MZ films loaded with varying concentrations (2.5%-10%) of GS and MZ. 600x magnification. Images presented here are representative of the samples.

biopolymers as effective carriers for local drug delivery (Thatte et al., 2005). In particular, polycaprolactone (PCL) is commonly used in tissue engineering (Ng et al., 2007; Ashton et al., 2011; Neves et al., 2011; Siddiqui et al., 2018) and drug delivery applications (Woodruff and Hutmacher, 2010). We extend upon these research themes by using a solvent-free, powder processing method to meld PCL with customizable payloads. The process involves cryogenic attrition of PCL to obtain fine particulate powders, which can subsequently be blended with high concentrations of additives, and finally fused into a variety of configurations (Lim et al., 2014). Here, we studied the incorporation of two antibiotics: gentamicin sulfate (GS) and metronidazole (MZ). Gentamicin was chosen as it is an established antibiotic that can inhibit and/or kill bacteria of most typical post-surgical infections [16]. MZ was also selected as it was a drug of clinical significance in combating anaerobic infections (Brook, 2016). Together, these two antibiotics target a wide antibacterial spectrum. GS and MZ were mixed with PCL powders and heat pressed to form PCL/GS and PCL/MZ films of varying antibiotic compositions. These films were then characterized on mechanical properties and surface topographies. Elution

assays were performed in vitro to evaluate drug release profile, and functional evaluations of antibacterial effectiveness and cytocompatibility were performed. Our results suggest the potential utility of this fabrication approach antibiotic-loaded scaffold.

## RESULTS

### Surface morphology of films

Figure 1 shows the SEM images of PCL (control) and GS/MZ powder and samples of different GS/MZ compositions ranging from 2.5-10% incorporated into PCL. GS and MZ are very different in terms of their geometry when in powder form but are absent when incorporated into PCL. At concentrations of 2.5% and 5% GS films were largely featureless and indistinguishable from native PCL films. Pitting was evident at concentrations of 10%. PCL/MZ surfaces were observed to contain minimal aggregates at concentrations of 2.5% and 5%. Unlike PCL/GS, hardly any morphological defects were observed at 10% MZ.

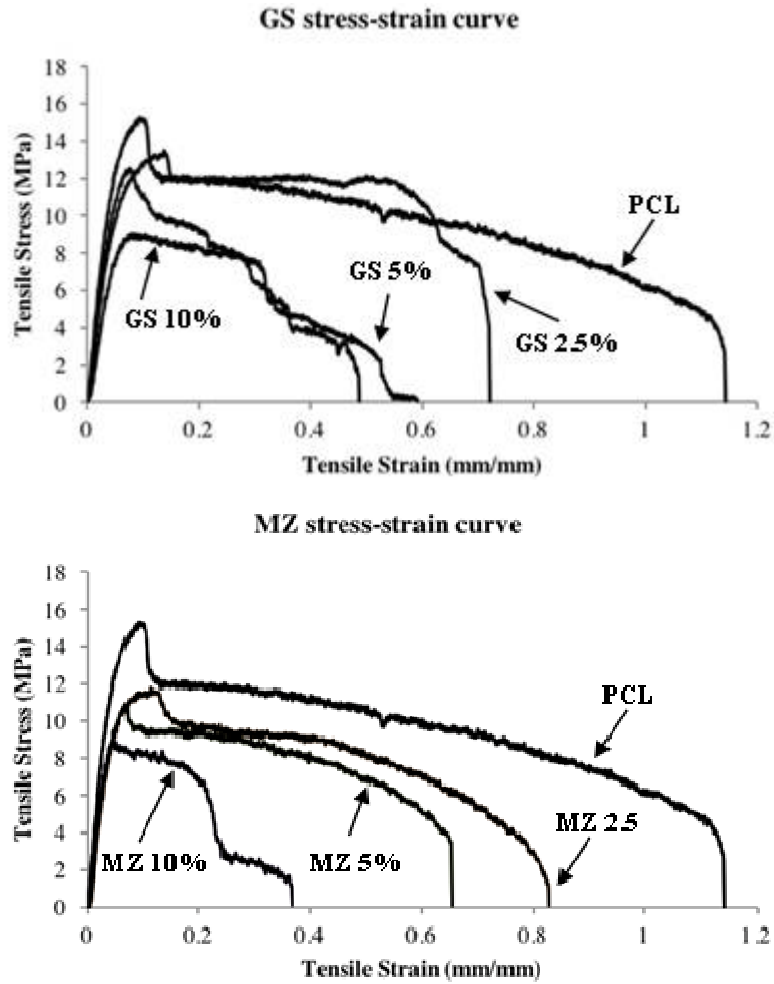


Figure 2a

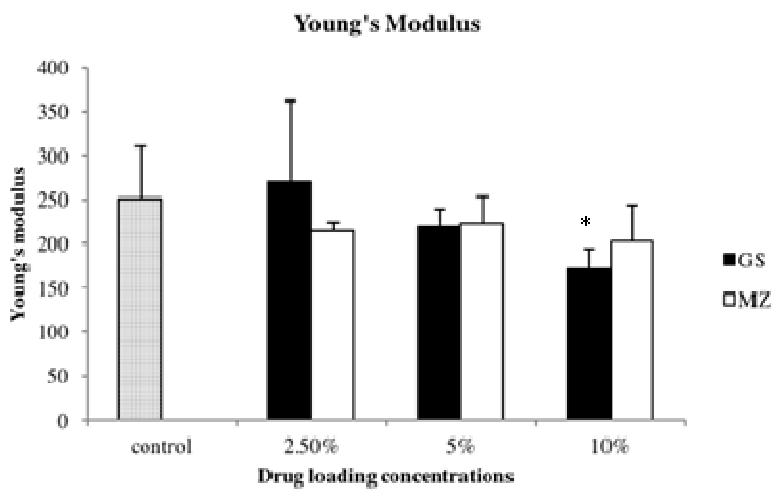


Figure 2b

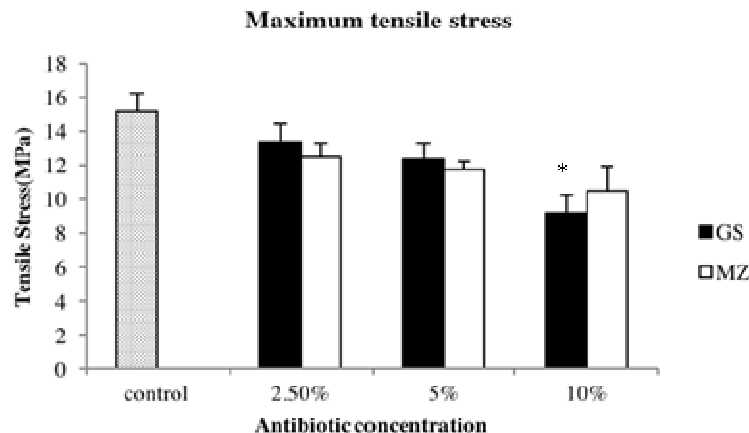


Figure 2c

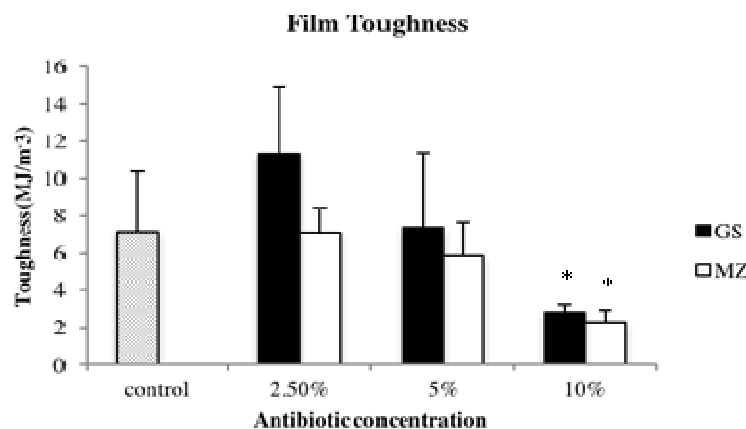


Figure 2d

**Figure 2.** Mechanical properties of films with varying antibiotic compositions (a) Stress-Strain curves (b) Young's Modulus (c) Maximum tensile stress (d) Toughness. \* denotes  $p < 0.05$  as compared to control (PCL) film.

### Mechanical properties of films

Mechanical properties of PCL/GS and PCL/MZ were evaluated by tensile testing and shown in Figure 2. Figure 2a shows the typical stress-strain curve for both the PCL/GS and PCL/MZ films. The antibiotic concentrations of 10% were found to compromise mechanical properties. In comparing Young's moduli, increased concentrations of GS were associated with decreased stiffness (figure 2b). PCL/MZ films however, appeared independent of antibiotic concentration, with Young's moduli in the range of 200 to 250MPa. Tensile strength was reduced by increased antibiotic load in both groups, but less appreciably in PCL/MZ groups (figure 2c). PCL had the highest tensile strength of 13.88MPa and gradually decreased as antibiotic concentration increased. Interestingly, PCL/GS shows increased toughness at 2.5% ( $11.3\text{MJ/m}^3$ ), followed by a sharp decrease at higher concentrations to  $2.8\text{MJ/m}^3$  at GS concentrations of 10% (figure 2d). PCL/MZ had a

toughness of  $7.1\text{MJ/m}^3$  at 2.5% (similar to PCL) and subsequently decreased at higher MZ concentrations.

### *In vitro* drug release profiles of films

GS and MZ release was plotted as concentration against time (Figure 3). A burst release of GS observed within the first 4 hours. Thereafter, this was followed by a sustained and prolonged release. For MZ, figure 3b shows the release profile of films from 0 to 192 hours plotted as a function of concentration against time. There was no detectable MZ drug release for 2.5%. Films with concentrations of 5% and 10% had a burst release of metronidazole within day 1, followed by a sustained and prolonged release for the next 7 days. In general, this burst release is similar to that observed in GS films whereby the initial release at the first day was the highest.

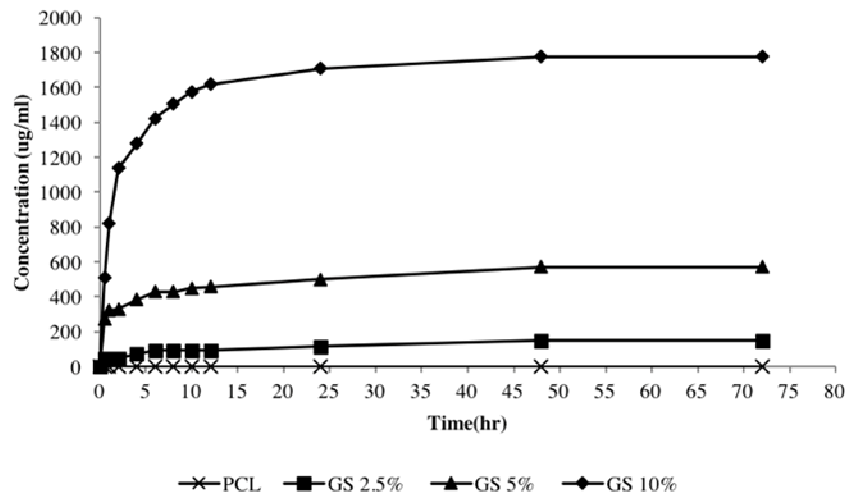


Figure 3a

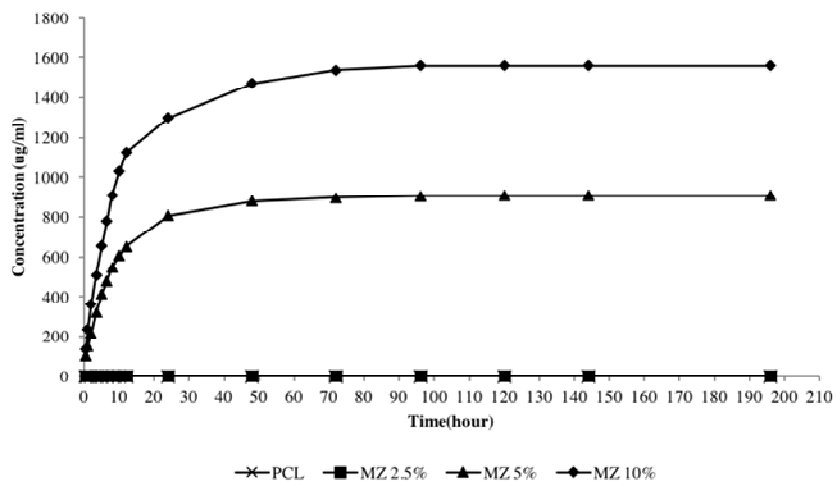


Figure 3b

**Figure 3.** Release profiles of films over time of (a) PCL-GS and (b) PCL-MZ. Cumulative drug release was represented in terms of concentration ( $\mu\text{g/ml}$ ) over time.

### Antimicrobial testing

Antibiotics-laden PCL films were placed on a bacterial lawn and the zone of inhibition (ZOI) was examined and compared against that of standard antibiotic discs (Figure 4). The ZOI in the control, commercially available standards and the respective concentrations were without any secondary regrowth and could be clearly seen (Figure 4a, b, c). From figure 4d, the ZOI on *P. aeruginosa* increased as the GS concentration increased with 10% having the largest mean ZOI (approx. 32mm). In contrast, when tested on *S. aureus*, there was a gradual increase in ZOI with increasing GS concentrations and 10% GS had a ZOI of about 23mm. It was also observed that no ZOI was seen around the PCL

films, demonstrating that it does not suppress *P. aeruginosa* nor *S. aureus* growth (Figure 4a, b).

For MZ, anaerobic *C. sporogenes* was used as the test organism. The PCL film by itself did not inhibit *C. sporogenes* growth. Commercial standards of MZ 5 $\mu\text{g}$  and 50 $\mu\text{g}$  were used for benchmarking purposes. From figure 4e, there is a dose-dependent increase in the ZOI with 10% having the largest mean ZOI (approx. 70mm) and showing the most significant microbial inhibition of all the samples tested.

### Cytocompatibility and effect on cell metabolism

Although the antibiotics had inhibitive effects on bacteria,

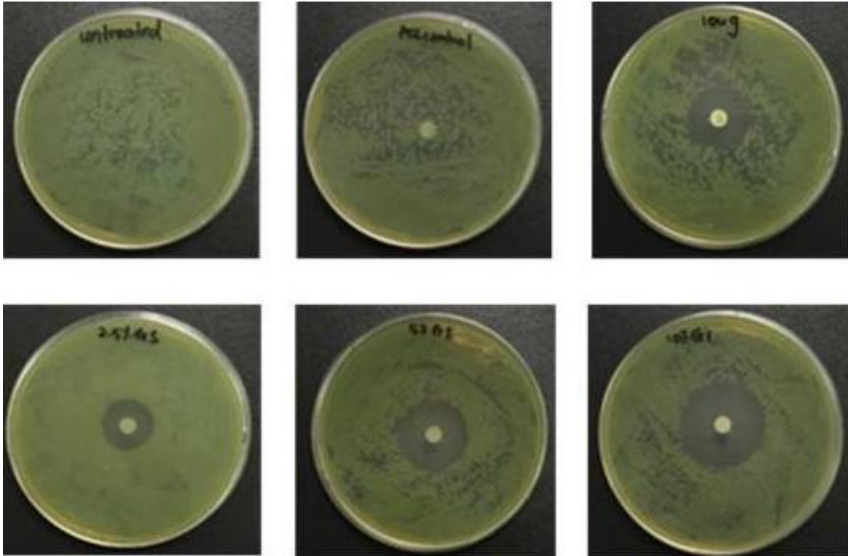


Figure 4a

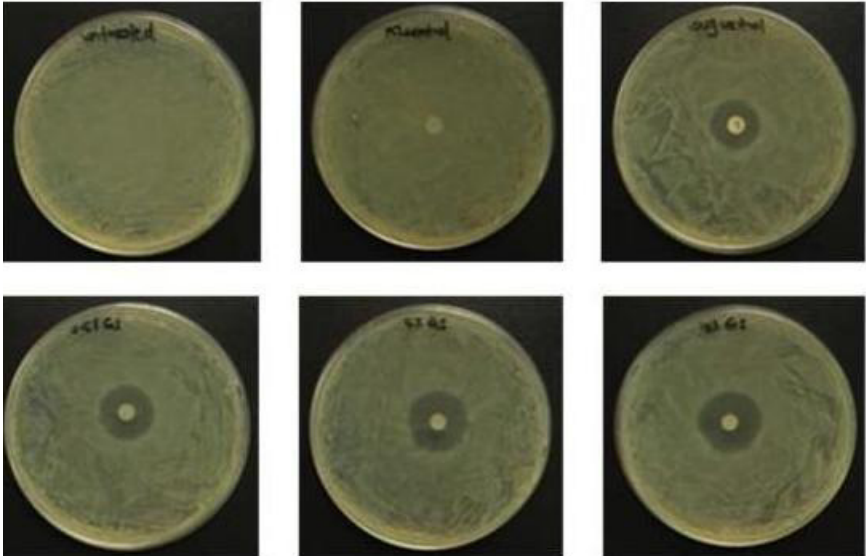


Figure 4b

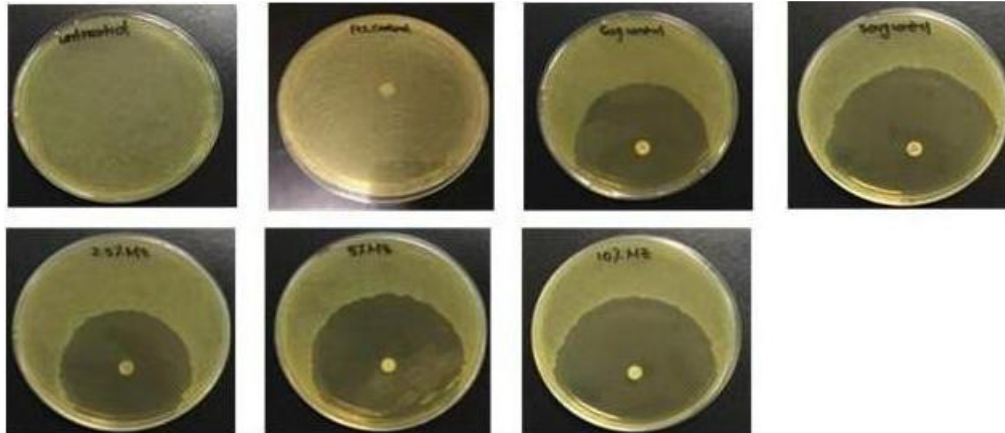


Figure 4c

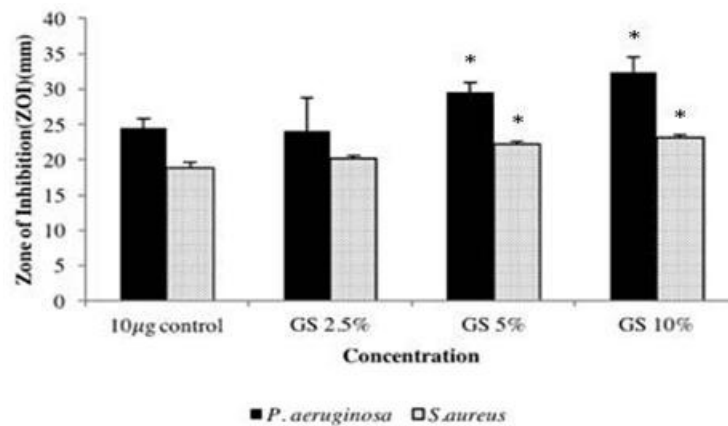


Figure 4d

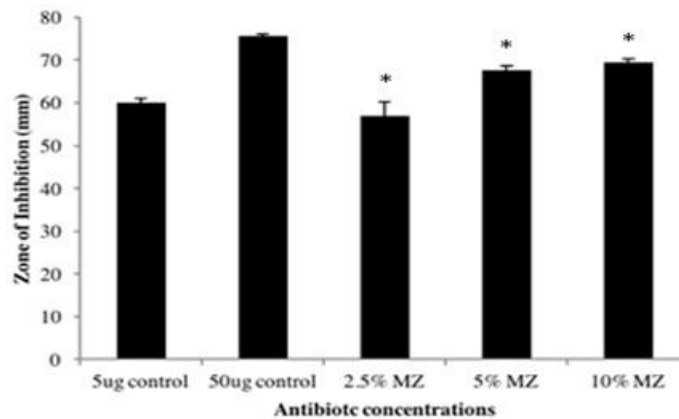


Figure 4e

**Figure 4.** Inhibitory effects of films against bacteria. (a) ZOI of PCL-GS on *P. aeruginosa* (b) ZOI of PCL-GS on *S. aureus* (c) ZOI of PCL-MZ on *C. sporogenes*. (d, e) Quantification of ZOI data of PCL-GS and PCL-MZ respectively. \* denotes  $p < 0.05$  as compared to 10µg standard control for GS and 5µg and 50µg standard controls for MZ.

their toxicity and metabolism on cells have yet to be evaluated. In this part of study, the effects of the films

were examined through viability staining and Alamar blue assay on fibroblasts (Figure 5). From Figure 5a, on day 1,

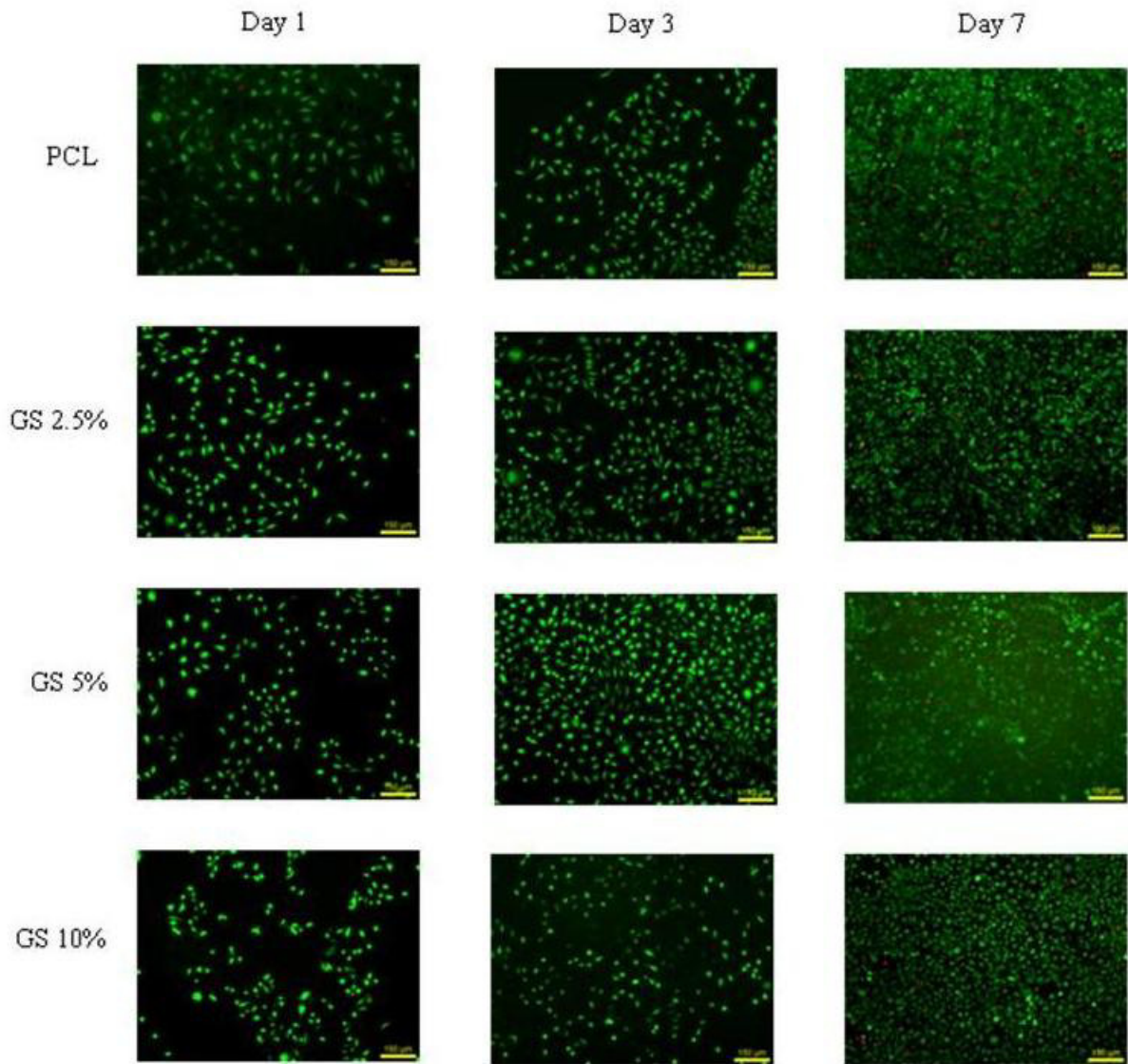


Figure 5a

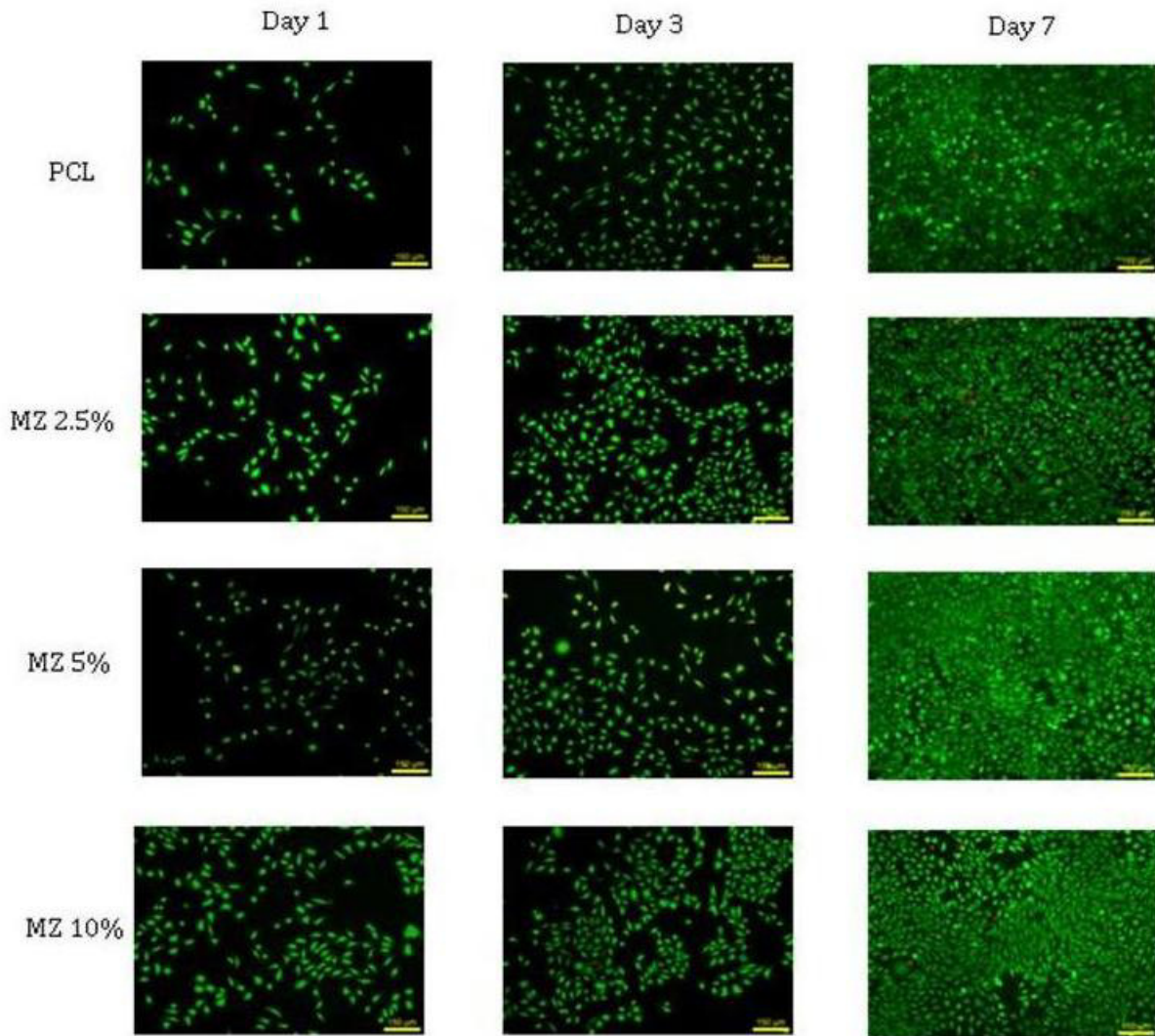


Figure 5b

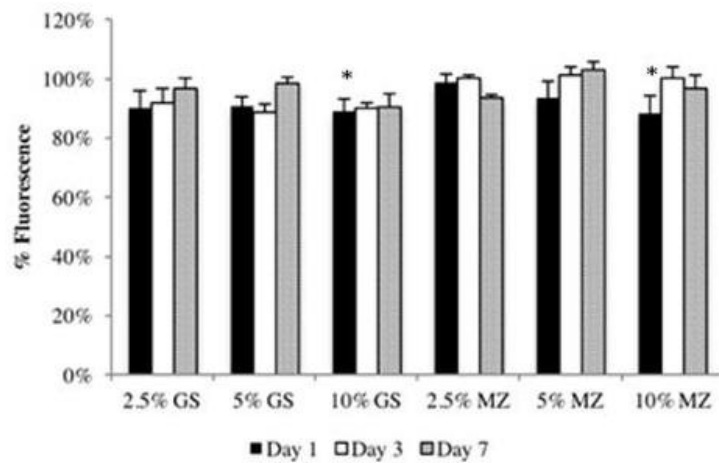


Figure 5c

**Figure 5.** Film cytotoxicity over 7 days with varying concentrations of GS and MZ on PCL films (a, b) viability staining and (c) Alamar blue. Images a) and b) presented here are representative of the sample. Viability staining data is normalized to that of PCL film only with 100% being the value of PCL. \* denotes  $p < 0.05$  as compared to PCL at corresponding time points.

the cells showed good adhesion in all concentrations of GS and MZ. By days 3 and 7, cell growth was unaffected and comparable to levels of that of the PCL control. All concentrations showed evidence of an increase in cell adhesion and proliferation between day 1 and 3. To quantitatively evaluate cellular health, Alamar blue was used. The cells exposed to both 10% PCL/GS and PCL/MZ showed significant differences in viability at day 1 when compared to PCL. Interestingly, at the highest concentration of 10% GS, no significant difference was observed. From day 3 onwards, all the cells irrespective of GS concentration report an increase in the fluorescence. In the PCL/MZ samples, 10% MZ revealed an initial drop in the viability as compared to the PCL control. However, this decrease was reversed when incubated for longer periods.

## DISCUSSION

Osteomyelitis and many other post-operational tissue infections, such as musculoskeletal and periodontal infections remains a major and serious problem for both patients and doctors (Spagnolo et al., 1993)

19. (Stevens et al., 2005; Virto et al., 2007; Moskowitz et al., 2010). These infections prolong pain and suffering to patients and carries with it a financial burden as well. More distressingly, patients may succumb to renewed disabilities and, in some cases, even death if these infections are not well treated (Lew and Waldvogel, 2004). The development of infections can be associated to pathogenic microbes such as *S. aureus*, *P. aeruginosa* and *Clostridia* species (Langer and Peppas, 2003; Chatterjee et al., 2016; Akhi et al., 2015). Antibiotic therapy represents an important step in dealing with infections associated with such microbes conventionally through systemic administration (Wu et al., 2013). These are, however, associated with systemic toxicity and poor bio-distribution to the compromised wound site. To address this, infected tissue is removed, and antibiotic-incorporated PMMA void fillers are currently implanted as bone spacers in the interim period prior to revision surgery, in order to remove residual infections (Naraharisetti et al., 2006; Liu and Chang, 2009; Inzana et al., 2016). Impracticalities of this approach include offloading of the affected limbs for extended periods and the need for multiple surgeries (Lim et al., 2014; Langer and Peppas, 2003). Bioresorbable drug delivery systems may provide solutions, both as a prophylactic coating for implants and as bioresorbable implants in themselves. Desirable features of such a system would include the capacity to incorporate customizable payloads of a wide range of antibiotic combinations and concentrations (Acharya et al., 2010). PCL has flexible mechanical properties that make it amendable for clinical applications such as wound dressings, contraceptives and for use in dentistry (Woodruff and Huttmacher, 2010; Mas Estelles

et al., 2008). Hydrogels although able to coat surface of complex geometry and are easy to apply, there is minimal control over loading efficacy and release kinetics (Goodman et al., 2013).

In our previous study, we had demonstrated powder processing to be an efficient, solvent-free method to dope large quantities of pharmaceutical agents into a PCL matrix (Allaf et al., 2013). Here, we evaluated this approach as a means to generate PCL matrices with even distribution of antibiotic load for sustained and controlled deliveries. Although not an injectable, we envision that this can be used as implanted scaffold or implant coatings.

## Morphology and mechanical properties of PCL/GS and PCL/MZ films

From the micrographs shown in figure 1, the incorporation of GS particles resulted in noticeable morphological changes, particularly at the higher concentration of 10%. These fusion defects may have arisen from local aggregation of the dopant in the PCL melt-phase, and subsequent micro-spalling leading to pit formation. With respect to MZ, no significant changes in film morphology were observed under SEM. At higher MZ concentrations, some fibrous, porous structures started to become evident. Similar to that of GS, these may be attributed to aggregation; the less pronounced effects are likely due to the more polar nature of MZ and, hence, better dispersion in the polymer matrix.

For both PCL/GS and PCL/MZ, the data demonstrates a general decrease in Young's modulus across the concentrations, ensuring flexibility maintained and importantly also indicates that the stiffness of PCL would not be greatly increased by the incorporation of various GS/MZ concentrations. Generally, antimicrobial films that are flexible would be greatly favourable to be used as a drug delivery platform. This is so as films would be able to conform to shape and be easy to handle for potential applications (Chen et al., 2014).

When toughness is examined, the results demonstrate that the pores in 2.5% GS and 5% GS as seen in the SEM images do not affect the resilience of the material. The possible strengthening of toughness could be explained by the location, shape and size of pores at or near the crack location (Leguillon and Piat, 2008). Crack blunting could have occurred in 2.5% GS and 5% GS resulting in enhancement of toughness. This is possible as a single pore at the tip of the crack could have increased its apparent toughness, with the larger the pore the larger the enhancement [35, 36]. Moreover, the smaller pore sizes in lower concentrations could have had greater specific surface and interfacial areas within the matrix, leading to an increase in toughness (Razak, 2012). With respect to MZ, there is no significant difference in toughness deviation in toughness of 2.5%

and 5% as compared to PCL. This shows that 2.5% of MZ incorporated would be able to have similar deformation and withstand pressures similar to PCL if the films were implanted in animal models. At higher concentrations of GS and MZ, their toughness is significantly reduced and are less malleable. However, when used as an implant coating, the mechanical properties become may not be as crucial as its primary role is to address potential infection at the tissue-implant interface.

### Drug release profile

Interestingly, it was shown that GS 10% film released the highest amount of antibiotics (55%) in terms of concentration (1600µg/ml) and total percentage cumulative amount when compared with the other concentrations. A major contributing factor to this finding could be due to the different pore structure present on the 10% film surface when compared to the rest of the concentrations as observed in the SEM micrographs. In addition, the pore structures of 2.5% and 5% seem to occur less frequently, possibly resulting in lower levels of dissolution when immersed in PBS. MZ 2.5% release could not be detected as it was below the detection limits. Similar to what was observed in GS/PCL, at higher concentrations of MZ, less cumulative antibiotic was released. This can be explained by the entrapment of MZ in PCL during fabrication as observed in the SEM micrographs. It is conceivable that bulk degradation of PCL would have to occur first before the entrapped MZ can be released. It must be highlighted that a burst release was observed and completed 4 hours after initial immersion into DI water. This initial burst is necessary for drug delivery platforms as a high drug dose is normally required during the initial period, to combat bacterial infections effectively and then slowly prolong the release for longer time periods to complete the treatment (Balmayor et al., 2012). Such elution profiles are desirable in infection control applications, as it features a short duration of antibiotic release without sub-inhibitory GS concentrations that brings about resistant strains (van de Belt et al., 1999). Also, as the inflammatory response to wound healing (acute phase) occurs in the initial 24-48 hours (Busti et al., 2005), having a burst release may prevent the initial attachment and subsequent biofilm formation leading to lowered infection risk better healing at the infection site. An early prevention in the biofilm formation will greatly benefit the healing of wound, due to the dramatic increase of up to 10-1000 times more resistance to antimicrobial agents as compared to the planktonic counterparts (Hoyle and Costerton (1991). Generally, biofilm infections will not clear until the implant has been removed and re-implantation after removal of an infected joint replacement has a high failure rate (Neut

et al., 2005).

In the experiment conducted, the main driving factors for in vitro drug release could be due to the presence of a diffusion gradient as the films were fully submerged in DI water, solubility of GS/MZ in water, as well as solute diffusion through the pores present within the matrix. Degradation is often one of a major driving force for drug release kinetics however this has been proven to be not so for polymer matrixes consisting of PCL (Arifin et al., 2006). This is because PCL is a slow degrading material which takes over two years to be completely degraded under physiological conditions (Lao et al., 2008). These characteristics may prove beneficial in the treatment of infections for long periods. Due to the short-release profiles of current anti-microbial materials, there is increasing interest in immobilization of antibiotics/antimicrobial peptides to the implant surface by permanent covalent tethering for long-term prevention of implant-associated infections (Hickok and Shapiro, 2012).

### Antimicrobial activity

Ideal local antibiotic delivery systems should provide reliable pathogen killing via an immediate burst release within the first 24-hour period after administration followed by sustained drug release above the tissue bed's minimal inhibitory concentration (MIC) to address the remaining microbial threat out to a 6-to-8-week time point asserted by the orthopedic community as an important point for infection prevention (Kanellakopoulou and Giamarellos-Bourboulis, 2000). In this work, the results from the bacteria assay confirmed that both GS and MZ did not lose their antimicrobial properties after fabrication. The ZOI between *P. aeruginosa* and *S. aureus* were different but this was to be expected as these are two different bacterial species. The ZOI exhibited a dose-dependent increase in GS concentration although the increase of ZOI was less pronounced for *S. aureus*. This may be due to the fact that an increase in GS may not necessarily translate to an increase in bacterial killing (Tam et al., 2006). For MZ, 5% and 10% showed similar levels of ZOIs suggesting that there is no dose dependent release of MZ into the agar. This is in agreement with the observed release profiles of MZ which reveal that at higher concentrations, this is reduced. Nevertheless, the MZ data validates the antimicrobial ability of the film. In all, antibiotics together with PCL blended using cryomilling not only demonstrate the ability for sustained release but antimicrobial efficacy against bacteria. The comparison with commercially available antibiotic discs corroborates the potency of the antibiotic loaded PCL films and is crucial in analyzing its effectiveness as a drug delivery vehicle.

### ***In vitro* compatibility**

While antibiotics are largely specific in their targets, accumulation and exposure to excessive doses may be cytotoxic, leading to unexpected cell death and tissue necrosis, further compromising the surgical site. To evaluate potential cytotoxicity, fibroblasts were incubated together with the liquid extracts of the films and cell viability assessed. To note, despite the increase in antibiotic concentrations, there was no observable and quantitative effect on the viability of the cells. Our results suggest normal cellular proliferation in the presence of films, with no obvious signs of cell death.

### **Experimental Section**

**Materials:** Gentamicin Sulfate (GS) Salt (Sigma, St Louis, MO) with a melting temperature range of 218-237 °C and Metronidazole (MZ) (Sigma, St Louis, MO) with a melting temperature range of 159-161 °C were used as-obtained. Medical grade poly ( $\epsilon$ -caprolactone) (PCL) pellets (Osteopore International, Singapore) with a melting temperature range of 58-60 °C was used in this study (Lim et al., 2014).

**Cryomilling of PCL pellets:** PCL pellets were cryomilled (Cryomill, Retsch, Germany) into PCL powder with a cryomilling cycle of 5-minutes precooling and 50-minutes of continuous milling. Thereafter, PCL/GS and PCL/MZ composites were homogeneously formed through the same process. Briefly, GS and MZ of different proportions (2.5%, 5% and 10%) with respect to PCL were loaded into a cryogenic vial with a ball-to-mass ratio of 30:1. The cryomilling period was 5-minutes of precooling at a cryogenic temperature (approx. -196°C) and 20 minutes of continuous milling at a frequency of 17.5 Hz.

**Heat Pressing of Films:** Uniformly blended PCL/GS and PCL/MZ powders of different proportions were thermally pressed into films with an approximate thickness of 100-120 $\mu$ m. 0.5g of the blend was placed in between two 0.1mm aluminum sheets and heat pressed (Carver 3853, Wabash, USA). Temperature of the Carver System was maintained at 80 °C for 15 minutes and allowed to cool by natural convection for 1 hour. Pressure was maintained at 0.158MPa throughout the pressing and cooling process. Thereafter, films were removed from the aluminum sheets using minimal water and force and stored in a cabinet with humidity control (DigiCabi, AD-100, Singapore).

**Mechanical properties of films:** The mechanical characteristics of PCL/GS and PCL/MZ films were determined using tensile tests (Instron tester 5569, USA) with a 1kN load cell. Films of each composition were cut into 5cm x 1cm rectangular strips and mounted onto a 5cm x 5cm paper frame with gauge length of 3cm. The rate of elongation was 3mm/min (10% of gauge length).

The sample thickness of each composition was determined by measuring 6 points using a micrometer (Coolant Proof Micrometer, IP65, Mitutoyo, Japan) and then calculating the average thickness. All experiments were conducted with a sample size of n=6. The analysis of mechanical properties was done using the stress-strain curve through the calculation of Young's modulus (stiffness), toughness and maximum tensile strength. Young's modulus was attained by way of the secant modulus method. Toughness was approximated by the area under the stress-strain curve with the use of the trapezium rule:  $Area = \sum \frac{Y_1+Y_2}{2} \times (X_2 - X_1) J/cm^3$

**Film morphology:** PCL/GS and PCL/MZ films were placed in the JFC-1600 Autofine Coater (JEOL, Japan) to be coated with platinum for 60 seconds at 20mA. Thereafter the surface morphologies of the samples were observed using a Scanning Electron Microscope (SEM) (JSM-6390LA, Jeol, Japan) with an acceleration voltage of 10kV.

***In vitro* drug release:** *In vitro* drug release for PCL/GS films were assayed using a protocol adapted from Teo et al. (2011). For each composition, 3 film samples of total weight 30mg were pre-treated with 3M NaOH for 1 hour and washed in Phosphate Buffer Saline (PBS) at room temperature and transferred into new vial of containing 1ml PBS for a range of time intervals. Prior to GS absorbance analysis, an o-phthalaldehyde reagent was made using 0.5 g of o-phthalaldehyde, 12.5 ml of methanol and 0.6 ml of 2-hydroxy-ethylmercaptan and 112 ml of 0.04 M sodium borate in distilled water. For GS analysis, 200ul of o-phthalaldehyde reagent and 200ul of isopropanol were added to 200ul of test solution. Thereafter, the mixture was incubated in the dark for 45 minutes at room temperature. Absorbance was taken at 333nm. All readings were compared against a calibration curve generated from GS solutions of known concentrations.

Drug release studies for PCL/MZ films at different compositions were carried out. Similarly, for each composition, 3 film samples of total weight 30mg were pre-treated in 3M of NaOH for 1 hour and subsequently washed in deionized (DI) water. Samples were transferred to a new vial with 1ml water for a range of time intervals to measure the release of MZ. During these periods, samples were placed in room temperature on a shaker at 160rpm. MZ release was measured at an absorbance of 320nm with DI water as control. All readings were compared against a calibration curve generated from MZ solutions of known concentrations.

**Antimicrobial testing:** Ability of the samples to inhibit microbial growth was determined by a disc diffusion assay. *Staphylococcus aureus* (ATCC 25923) and *Pseudomonas aeruginosa* (PAO1) were the test organisms used for PCL/GS samples while *Clostridium sporogenes* (ATCC 13732) was used for PCL/MZ. Media preparations of broth and agar for reinforced Clostridial Medium (Oxoid, Basingstoke, UK) for PCL/MZ samples

and Mueller-Hinton (Oxoid, Basingstoke, UK) for PCL/GS samples) were prepared in advance. In addition, 6mm PCL/GS and PCL/MZ samples were punched out using a biopsy punch and sterilized using 100% ethanol. Broth cultures were prepared with an overnight inoculation for *S. aureus* and *P. aeruginosa* and 3 days for *C. sporogenes*. All cultures were incubated at 37°C and for *C. sporogenes*, an anaerobic Gaspak (Becton, Dickinson and Company) was used. After incubation, an optical density (600nm) (Molecular Devices, SpectraMax) of approximately 0.15 for *S. aureus* and *P. aeruginosa* and approximately 0.20 for *C. sporogenes* was obtained. 100µl of culture was spread uniformly onto the surface of the respective agar using a spreader to form a bacterial lawn. Thereafter a sterile 6mm sample was placed gently on top of the agar and the plates were incubated for 1 day for (*S. aureus* and *P. aeruginosa*) and 3 days (*C. sporogenes*). Thereafter, the zones of inhibition (defined as the diameter of the zone with no bacterial growth taken across the sample) were measured and compared to that of commercial available discs of GS (10ug) and MZ (5ug and 50ug) (Oxoid, Basingstoke, UK).

**Cell culture:** Fibroblasts (L929) are used to in the cytocompatibility and cytotoxicity studies. Cells are cultured in DMEM (ThermoFisher, Waltham, USA) with 10% fetal bovine serum (ThermoFisher, Waltham, USA) at 37°C.

**Cytocompatibility:** The cell viability when exposed to PCL/GS and PCL/MZ over time was determined via indirect testing accordingly to the methods adapted from ISO 10993-5 standards. Samples were disinfected by soaking in 100% ethanol for 24 hours and washed with sterile phosphate buffer saline before use. They were then left to incubate overnight in 1ml of culture media and the supernatant was filtered and used for testing. L929 cells (mouse fibroblasts) were seeded in 12-well plates at a density of 10,000 cells/cm<sup>2</sup> and incubated together with the sample supernatant. On days 1, 3 and 7, viability assay using fluorescein diacetate (FDA)/ propidium iodide (PI) (Life Technologies, California, USA) was performed and images were taken using fluorescence microscopy (Olympus FV-1000).

**Cytotoxicity:** Cell metabolism effects were determined using Alamar Blue (Life Technologies, California, USA). PCL/GS and PCL/MZ samples were prepared similarly as the cytocompatibility study. L929 cells with a density of 10,000 cells/cm<sup>2</sup> were seeded into 12-well plates and incubated together with the sample supernatant. On days 1, 3 and 7, alamar blue was added to the culture media in a ratio of 1:10 and incubated for 3 hours. Aliquots of 200ul each were prepared in a 96-well plate and measured for florescence at an excitation /emission wavelength of 560nm/590nm using a spectrophotometer (SpectraMax, Molecular Devices).

## CONCLUSION

Topical delivery via drug carriers may be used to overcome the limited bioavailability of antibiotics associated with oral or transdermal routes of administration due to its poor intestinal and dermal permeability [47]. Moreover, the general concern about risk of over toxicity and systemic toxicity can also be avoided when low concentrations incorporated can be released locally, targeting only the infection site [48]. Furthermore, GS belong to the heat-stable family of aminoglycosides and is thermally stable [49]. The same can be said of MZ as well [50] and thus both these antibiotics are compatible with a range of fabrication and incorporation methods, including heat-pressed films. Tailoring antibiotic release bioactivity using antibiotic-polymer miscibility provides extended, antibiotic delivery that can be customized and combined to meet established criteria and accommodate diverse clinical needs while better addressing antibiotic-resistance [51, 52]. This study demonstrates the ability of a synthetic biodegradable polymer that when loaded with antibiotics will be able to provide a localized antimicrobial effect that has potential for use in implant surgery.

## ACKNOWLEDGEMENTS

Financial support for this research was provided by NTU Internal Funding (M4081390), MOE2016-T2-2-108 and IAF PP- H17/01/a0/0S9.

## Conflict of Interest Disclosure

The authors declare no competing financial interest.

## REFERENCES

- Acharya G, CS Shin, K. Vedantham, M. McDermott, T. Rish, K. Hansen, Y. Fu, K. Park (2010). A study of drug release from homogeneous PLGA microstructures. *J Control Release*, 146(2): p. 201-6.
- Akhi MT, R. Ghotaslou, S. Beheshtirouy, M. Asgharzadeh, T. Pirzadeh, B. Asghari, N. Alizadeh, A. Toloue Ostadgavahi, V. Sorayaei Somesaraei, M.Y. Memar (2015). Antibiotic Susceptibility Pattern of Aerobic and Anaerobic Bacteria Isolated From Surgical Site Infection of Hospitalized Patients. *Jundishapur J Microbiol*, 8(7): p. e20309.
- Allaf RM, I.V. Rivero, N. Abidi, and I.N. Ivanov (2013). Porous poly(epsilon-caprolactone) scaffolds for load-bearing tissue regeneration: solventless fabrication and characterization. *J Biomed Mater Res B Appl Biomater*, 101(6): p. 1050-60.
- Arifin DY, L.Y. Lee, and C.H. Wang (2006). Mathematical modeling and simulation of drug release from microspheres: Implications to drug delivery systems. *Adv Drug Deliv Rev*, 58(12-13): p. 1274-325.
- Aronson NE, JW. Sanders, and K.A. Moran (2006). In harm's way: infections in deployed American military forces. *Clin Infect Dis*, 43(8): p. 1045-51.
- Ashton JH., J.A. Mertz, J.L. Harper, M.J. Slepian, J.L. Mills, D.V. McGrath, and J.P. Vande Geest (2011). Polymeric endoaortic paving: Mechanical, thermoforming, and degradation properties of

- polycaprolactone/polyurethane blends for cardiovascular applications. *Acta Biomater*, 7(1): p. 287-94.
- Bailey SR. (1997). Local drug delivery: current applications. *Prog Cardiovasc Dis*, 40(2): p. 183-204.
- Balmayor ER, E.T. Baran, H.S. Azevedo, and R.L. Reis (2012). Injectable biodegradable starch/chitosan delivery system for the sustained release of gentamicin to treat bone infections. *Carbohydrate Polymers*, 87(1): p. 32-39.
- Brook I (2016). Spectrum and treatment of anaerobic infections. *J Infect Chemother*, 22(1): p. 1-13.
- Brooks, B.D., S.N. Davidoff, D.W. Grainger, and A.E. Brooks (2013). Comparisons of release of several antibiotics from antimicrobial polymer-coated allograft bone void filler. *Int J Biomed Mater Res*, 1: p. 21-25.
- Busti A.J., J.S. Hooper, C.J. Amaya, and S. Kazi (2005). Effects of perioperative antiinflammatory and immunomodulating therapy on surgical wound healing. *Pharmacotherapy*, 25(11): p. 1566-91.
- Chatterjee, M., C.P. Anju, L. Biswas, V. Anil Kumar, C. Gopi Mohan, and R. Biswas (2016). Antibiotic resistance in *Pseudomonas aeruginosa* and alternative therapeutic options. *Int J Med Microbiol*, 306(1): p. 48-58.
- Chen, D., M. Wu, J. Chen, C. Zhang, T. Pan, B. Zhang, H. Tian, X. Chen, and J. Sun (2014). Robust, flexible, and bioadhesive free-standing films for the co-delivery of antibiotics and growth factors. *Langmuir*, 30(46): p. 13898-906.
- Coello, R., A. Charlett, J. Wilson, V. Ward, A. Pearson, and P. Borriello (2005). Adverse impact of surgical site infections in English hospitals. *J Hosp Infect*, 60(2): p. 93-103.
- Goodman, S.B., Z. Yao, M. Keeney, and F. Yang (2013). The future of biologic coatings for orthopaedic implants. *Biomaterials*, 34(13): p. 3174-83.
- Griffis, C.D., S. Metcalfe, F.L. Bowling, A.J. Boulton, and D.G. Armstrong (2009). The use of gentamycin-impregnated foam in the management of diabetic foot infections: a promising delivery system? *Expert Opin Drug Deliv*, 6(6): p. 639-42.
- Hickok, N.J. and I.M. Shapiro (2012). Immobilized antibiotics to prevent orthopaedic implant infections. *Adv Drug Deliv Rev*, 64(12): p. 1165-76.
- Hoyle, B.D. and J.W. Costerton, *Bacterial resistance to antibiotics: The role of biofilms*, in *Progress in Drug Research / Fortschritte der Arzneimittelforschung / Progrès des recherches pharmaceutiques*, E. Jucker, Editor. 1991, Birkhäuser Basel: Basel. p. 91-105.
- Hui, T., X. Yongqing, Z. Tiane, L. Gang, Y. Yonggang, J. Muyao, L. Jun, and D. Jing (2009). Treatment of osteomyelitis by liposomal gentamicin-impregnated calcium sulfate. *Arch Orthop Trauma Surg*, 129(10): p. 1301-8.
- Inzana, J.A., E.M. Schwarz, S.L. Kates, and H.A. Awad (2016). Biomaterials approaches to treating implant-associated osteomyelitis. *Biomaterials*, 81: p. 58-71.
- Kanellakopoulou, K. and E.J. Giamarellos-Bourboulis (2000). Carrier systems for the local delivery of antibiotics in bone infections. *Drugs*, 59(6): p. 1223-32.
- Langer, R. and N.A. Peppas (2003). Advances in biomaterials, drug delivery, and bionanotechnology. *Aiche Journal*, 49(12): p. 2990-3006.
- Lao, L.L., S.S. Venkatraman, and N.A. Peppas (2008). Modeling of drug release from biodegradable polymer blends. *Eur J Pharm Biopharm*, 70(3): p. 796-803.
- Leguillon, D. and R. Piat (2008). Fracture of porous materials - Influence of the pore size. *Engineering Fracture Mechanics*, 75(7): p. 1840-1853.
- Lew, D.P. and F.A. Waldvogel (2004). Osteomyelitis. *Lancet*, 364(9431): p. 369-79.
- Lim, J., M.S. Chong, J.K. Chan, and S.H. Teoh (2014). Polymer powder processing of cryomilled polycaprolactone for solvent-free generation of homogeneous bioactive tissue engineering scaffolds. *Small*, 10(12): p. 2495-502.
- Liu, W.N. and J. Chang (2009). In vitro evaluation of gentamicin release from a bioactive tricalcium silicate bone cement. *Materials Science & Engineering C-Materials for Biological Applications*, 29(8): p. 2486-2492.
- Lucke, M., G. Schmidmaier, S. Sadoni, B. Wildemann, R. Schiller, N.P. Haas, and M. Raschke (2003). Gentamicin coating of metallic implants reduces implant-related osteomyelitis in rats. *Bone*, 32(5): p. 521-31.
- Mas Estelles, J., A. Vidaurre, J.M. Meseguer Duenas, and I. Castilla Cortazar (2008). Physical characterization of polycaprolactone scaffolds. *J Mater Sci Mater Med*, 19(1): p. 189-95.
- Moskowitz, J.S., M.R. Blaisse, R.E. Samuel, H.P. Hsu, M.B. Harris, S.D. Martin, J.C. Lee, M. Spector, and P.T. Hammond (2010). The effectiveness of the controlled release of gentamicin from polyelectrolyte multilayers in the treatment of *Staphylococcus aureus* infection in a rabbit bone model. *Biomaterials*, 31(23): p. 6019-30.
- Murray, C.K., S.A. Roop, D.R. Hospenthal, D.P. Dooley, K. Wenner, J. Hammock, N. Taufen, and E. Gouridine (2006). Bacteriology of war wounds at the time of injury. *Mil Med*, 171(9): p. 826-9.
- Naraharisetti, P.K., H.C. Guan Lee, Y.C. Fu, D.J. Lee, and C.H. Wang (2006). In vitro and in vivo release of gentamicin from biodegradable discs. *J Biomed Mater Res B Appl Biomater*, 77(2): p. 329-37.
- Neut, D., J.G. Hendriks, J.R. van Horn, H.C. van der Mei, and H.J. Busscher (2005). *Pseudomonas aeruginosa* biofilm formation and slime excretion on antibiotic-loaded bone cement. *Acta Orthop*, 76(1): p. 109-14.
- Neves, S.C., L.S. Moreira Teixeira, L. Moroni, R.L. Reis, C.A. Van Blitterswijk, N.M. Alves, M. Karperien, and J.F. Mano (2011). Chitosan/poly(epsilon-caprolactone) blend scaffolds for cartilage repair. *Biomaterials*, 32(4): p. 1068-79.
- Ng, K.W., H.N. Achuth, S. Moochhala, T.C. Lim, and D.W. Huttmacher (2007). In vivo evaluation of an ultra-thin polycaprolactone film as a wound dressing. *J Biomater Sci Polym Ed*, 18(7): p. 925-38.
- Noel, S.P., H. Courtney, J.D. Bumgardner, and W.O. Haggard (2008). Chitosan films: a potential local drug delivery system for antibiotics. *Clin Orthop Relat Res*, 466(6): p. 1377-82.
- Ragel, C.V. and M. Vallet-Regi (2000). In vitro bioactivity and gentamicin release from glass-polymer-antibiotic composites. *J Biomed Mater Res*, 51(3): p. 424-9.
- Razak, S.I.A., S. N., and R. W (2012). Biodegradable Polymers and their Bone Applications: A Review *Int J Basic Appl Sci*, 12(1): p. 31-49.
- Shiozuka, M., A. Wagatsuma, T. Kawamoto, H. Sasaki, K. Shimada, Y. Takahashi, Y. Nonomura, and R. Matsuda (2010). Transdermal delivery of a readthrough-inducing drug: a new approach of gentamicin administration for the treatment of nonsense mutation-mediated disorders. *J Biochem*, 147(4): p. 463-70.
- Siddiqui, N., S. Asawa, B. Birru, R. Baadhe, and S. Rao (2018). PCL-Based Composite Scaffold Matrices for Tissue Engineering Applications. *Mol Biotechnol*.
- Soares-Sobrinho, J.L., M.F. de La Roca Soares, P.Q. Lopes, L.P. Correia, F.S. de Souza, R.O. Macedo, and P.J. Rolim-Neto (2010). A preformulation study of a new medicine for Chagas disease treatment: physicochemical characterization, thermal stability, and compatibility of benznidazole. *AAPS PharmSciTech*, 11(3): p. 1391-6.
- Spagnolo, N., F. Greco, A. Rossi, L. Ciolli, A. Teti, and P. Posteraro (1993). Chronic staphylococcal osteomyelitis: a new experimental rat model. *Infect Immun*, 61(12): p. 5225-30.
- Stevens, D.L., A.L. Bisno, H.F. Chambers, E.D. Everett, P. Dellinger, E.J. Goldstein, S.L. Gorbach, J.V. Hirschmann, E.L. Kaplan, J.G. Montoya, and J.C. Wade (2005). Practice guidelines for the diagnosis and management of skin and soft-tissue infections. *Clin Infect Dis*, 41(10): p. 1373-406.
- Tam, V.H., S. Kabbara, G. Vo, A.N. Schilling, and E.A. Coyle (2006). Comparative pharmacodynamics of gentamicin against *Staphylococcus aureus* and *Pseudomonas aeruginosa*. *Antimicrob Agents Chemother*, 50(8): p. 2626-31.
- Teo EY, SY. Ong, M.S. Chong, Z. Zhang, J. Lu, S. Moochhala, B. Ho, and S.H. Teoh (2011). Polycaprolactone-based fused deposition modeled mesh for delivery of antibacterial agents to infected wounds. *Biomaterials*, 32(1): p. 279-87.
- Thatte, S., K. Datar, and R.M. Ottenbrite (2005). Perspectives On: Polymeric Drugs and Drug Delivery Systems. *Journal of Bioactive and Compatible Polymers*, 20(6): p. 585-601.

- Torres-Giner, S., A. Martinez-Abad, J.V. Gimeno-Alcaniz, M.J. Ocio, and J.M. Lagaron (2012). Controlled Delivery of Gentamicin Antibiotic from Bioactive Electrospun Polylactide-Based Ultrathin Fibers. *Advanced Engineering Materials*, 14(4): p. B112-B122.
- Traub, W.H. and B. Leonhard (1995). Heat stability of the antimicrobial activity of sixty-two antibacterial agents. *J Antimicrob Chemother*, 35(1): p. 149-54.
- van de Belt, H., D. Neut, J.R. van Horn, H.C. van der Mei, W. Schenk, and H.J. Busscher (1999). . . . or not to treat? *Nat Med*, 5(4): p. 358-9.
- Virto, M.R., B. Elorza, S. Torrado, L. Elorza Mde, and G. Frutos (2007). Improvement of gentamicin poly(D,L-lactic-co-glycolic acid) microspheres for treatment of osteomyelitis induced by orthopedic procedures. *Biomaterials*, 28(5): p. 877-85.
- Visscher, L.E., H.P. Dang, M.A. Knackstedt, D.W. Hutmacher, and P.A. Tran (2018). 3D printed Polycaprolactone scaffolds with dual macroporosity for applications in local delivery of antibiotics. *Mater Sci Eng C Mater Biol Appl*, 87: p. 78-89.
- Woodruff, M.A. and D.W. Hutmacher (2010). The return of a forgotten polymer-Polycaprolactone in the 21st century. *Progress in Polymer Science*, 35(10): p. 1217-1256.
- Wu, T., Q. Zhang, W. Ren, X. Yi, Z. Zhou, X. Peng, X. Yu, and M. Lang (2013). Controlled release of gentamicin from gelatin/genipin reinforced beta-tricalcium phosphate scaffold for the treatment of osteomyelitis. *Journal of Materials Chemistry B*, 1(26): p. 3304-3313.